arXiv:cond-mat/0605443v2 [cond-mat.mtrl-sci] 2 Aug 2006

Magnetically Mediated Transparent Conductors: In_2O_3 doped with Mo

J. E. Medvedeva*
Department of Physics, University of Missouri–Rolla, Rolla, MO 65409

First-principles band structure investigations of the electronic, optical and magnetic properties of Mo-doped In_2O_3 reveal the vital role of magnetic interactions in determining both the electrical conductivity and the Burstein-Moss shift which governs optical absorption. We demonstrate the advantages of the transition metal doping which results in smaller effective mass, larger fundamental band gap and better overall optical transmission in the visible – as compared to commercial Sn-doped In_2O_3. Similar behavior is expected upon doping with other transition metals opening up an avenue for the family of efficient transparent conductors mediated by magnetic interactions.

PACS number(s): 71.20.-b

A unique combination of high electrical conductivity and low optical absorption – a property which makes transparent conducting oxides (TCO) attractive for many advanced applications [1, 2, 3] – is well-known to be a challenge due to the mutual dependence of the optical transmission rates and conductivity. Among possible routes to avoid compromising the optical transparency [4, 5] is to enhance conductivity via mobility of the free carriers rather than their concentration. Recently, the mobility with more than twice the value of the typical commercial TCO materials such as Sn-doped indium oxide (ITO) was observed in Mo-doped In_2O_3 (IMO), and it was shown that the conductivity can be significantly increased with no changes in the spectral transmittance upon doping with Mo [6, 7, 8, 9]. Surprisingly, introduction of the transition metal Mo which donates two more carriers per substitution compared to Sn, does not lead to the expected increase of the optical absorption or a decrease of the mobility due to the scattering on the localized Mo d-states. Moreover, d-states of pre-transition metals (such as Sc and Y) were shown [10] to affect the band structure of the host TCO material by lowering the dispersion of the conduction band that, in turn, increases the effective mass and hence decreases the mobility. These inconsistencies call for in-depth theoretical analysis.

In this Letter, we present first-principles band structure investigations of the structural, electronic, optical and magnetic properties of Mo-doped In_2O_3 which reveal that the transition metal dopants can lead to the transport and optical properties competing with those of commercially utilized TCO. Most importantly, we find that the *magnetic interactions* which have never been considered to play a role in combining optical transparency with electrical conductivity, ensure both high carrier mobility and low optical absorption in the visible range. Compared to ITO, our results show that the magnetic exchange interaction splits the Mo d-states enabling (i) smaller increase of the effective mass; (ii) larger fundamental band gap; (iii) lower short-wavelength optical absorption; and (iv) lower plasma frequency and thus lower absorption in the long-wavelength range. We also demonstrate that strong sensitivity of the d-states of the dopant to its oxygen surrounding opens up a possibility to control the transport and optical properties with a proper d-element doping.

Approach. Full-potential linearized augmented plane wave method [11] with the local density approximation is employed [12] to study the electronic band structure of pure In_2O_3, ITO and IMO (both 6.25% doped), the latter with and without interstitial oxygen. For all systems containing Mo atoms, both non-spin-polarized and spin-polarized calculations were performed. The equilibrium relaxed geometry of all structures investigated was determined via the total energy and atomic forces minimization for the lattice parameter a and the internal atomic positions. During the optimization, all atoms were allowed to move in x, y and z directions. Less than 0.5% increase of the lattice parameter was found upon introduction of Mo and the interstitial oxygen, in agreement with experimental observations [6]. The Mo-O distances decrease by 4-20% as compared to the optimized In-O distances in pure In_2O_3.

Structural peculiarities. In_2O_3 has the ordered vacancy structure [13] with 8 formula units where four In atoms out of 16 occupy the centers of the trigonally distorted octahedra (denoted as In(1) position), while the rest are located at the centers of the tetragonally distorted octahedra (denoted as In(2)). From the total energy comparison of the structures with the Mo atom substituted into In(1) or In(2) sublattice, we found that Mo atoms prefer In(1) positions with the energy difference of 40 meV that is similar to ITO [14, 15]. However, in contrast to the Sn-doped case [14], the electronic structures of $Mo_{In(1)}$ and $Mo_{In(2)}$ systems are different. Clearly, the Mo d-states are more sensitive to the oxygen surrounding than the spherically-symmetric s-states of Sn atoms: we found that when Mo is in the trigonally distorted oxygen octahedron, the three t_{2g} levels are degenerate and cross the Fermi level (E_F), while they split by ∼0.8 eV into two occupied and one empty level in case of the tetragonal distortion of the Mo oxygen neighbors, cf., Figs. 1(a)

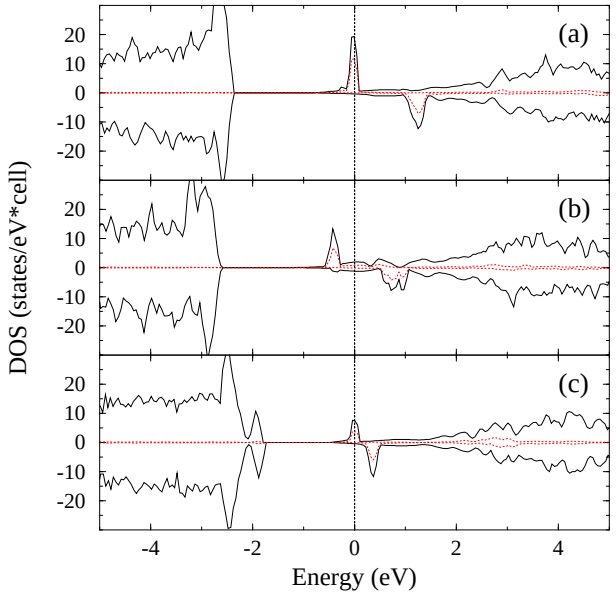

FIG. 1: Spin-resolved total (solid line) and Mo-4d (dashed line) density of states for (a) $Mo^{\bullet\bullet\bullet}_{In(1)}$, (b) $Mo^{\bullet\bullet\bullet}_{In(2)}$ and (c) $[Mo^{\bullet\bullet\bullet}_{In}O_i^{''}]^{\bullet}$ structures (see text for notations).

and 1(b). These findings may help elucidate the unusual observation that the carrier concentration decreases with temperature (for the systems grown with no ambient oxygen) which was not previously understood [8]. When the temperature is increased, the second substitutional site, i.e., $Mo_{In(2)}$, may become active. In this case, the density of states at E_F is significantly reduced (cf., Fig. 1(a) and 1(b)). Due to the splitting of the d-states, two of the three t_{2g} electrons become bound and cannot contribute to the charge transport.

Role of interstitial oxygen. To investigate the effect of interstitial oxygen on the structural, electronic and optical properties of IMO, we calculated the electronic band structure and the formation energies [16] of the systems with additional oxygen located at one of the vacancy positions near the dopant or In atoms. Using Kröger-Vink notation, the following complexes were considered in addition to the $Mo^{\bullet\bullet\bullet}_{In(1)}$ and $Mo^{\bullet\bullet\bullet}_{In(2)}$ defects: $[Mo^{\bullet\bullet\bullet}_{In(1)} + 2In_{In}O_i^{''}]^{\bullet}$ and $[Mo^{\bullet\bullet\bullet}_{In}O_i^{''}]^{\bullet}$, where the subscript stands for the site position and the superscript stands for effective negative ($'$) or positive ($\bullet$) charge. (Note, that we omit the site position subscript in the later complex since an interstitial oxygen makes the In(1) and In(2) positions equivalent by occupying one of the two available vacancy positions.) First, from a comparison of the formation energies, we found that the addition of oxygen results in the energy gain of ∼3 eV as compared to the structures without an interstitial oxygen, i.e., $Mo^{\bullet\bullet\bullet}_{In}$. This finding confirms previous predictions [6, 7, 9] that oxygen interstitials are likely to exist in IMO. We also found that O_i prefers to be located near the dopant rather than to be shared by two In atoms, forming $[2In_{In}O_i^{''}]^{\bullet}$ complex, with the energy difference of 1 eV.

Due to the high probability of the oxygen compensated complexes, one can expect a significant reduction of the ionized impurity scattering in IMO. Indeed, an increase of the relaxation time was observed when ambient oxygen content was increased during the deposition [8]. On the other hand, the interstitial oxygen significantly reduces the number of free carriers – from 3 to 1 per Mo substitution [17]. Thus, by varying the amount of oxygen one can concurrently control both the mobility (through the relaxation time) and free-carrier concentration. The highest electron concentration can be attained in samples grown in 100% Ar environment [8], i.e., without oxygen, while the relaxation time should be the shortest in this case and, moreover, it should rapidly decrease with Mo concentration since $Mo^{\bullet\bullet\bullet}_{In}$ is a strong scattering center. As the amount of oxygen increases, facilitating the formation of $[Mo^{\bullet\bullet\bullet}_{In}O_i^{''}]^{\bullet}$ complexes, the carrier concentration decreases [8, 9], whereas the mobility is improved due to the longer relaxation times. Thus, both intermediate dopant and oxygen concentrations will provide the optimum balance between carrier concentration and mobility resulting in the best transport properties of IMO. (Note that as our additional calculations showed [19], introduction of oxygen vacancies which may play an important role in samples grown with no oxygen ambient pressure does not affect the conclusions made in the current work.)

Role of magnetism. Most strikingly, we found that the magnetic configuration is considerably lower in energy as compared to the non-magnetic one, and Mo atoms possess a large magnetic moment (Table I) – despite the fact that Mo is not magnetic in bulk. Due to the strong exchange interactions, the Mo d-states located in the vicinity of E_F are split by about 1.3 eV and 0.4 eV for $Mo^{\bullet\bullet\bullet}_{In(1)}$ and $[Mo^{\bullet\bullet\bullet}_{In}O_i^{''}]^{\bullet}$, respectively, Figs. 1(a) and 1(c). To determine the magnetic coupling between two dopants, we performed calculations of Mo-doped In_2O_3 with doubled unit cell. The total energy difference between ferro- and antiferro-magnetic configurations for both $Mo^{\bullet\bullet\bullet}_{In(1)}$ and $[Mo^{\bullet\bullet\bullet}_{In}O_i^{''}]^{\bullet}$ is found to be negligible, ∼10 meV, suggesting a very weak magnetic coupling between the dopants which may result from the screening by the free carriers in the system [20].

It is important to note that the conductivity in IMO is due to the delocalized In s-states which form the highly disperse free-electron-like conduction band (cf., Fig. 2), while the Mo d-states are resonant states. The free carriers in the system flow in a background of the Mo defects which serve as strong scattering centers. Because of the exchange splitting of the Mo d-states, the carriers of one spin will be affected by only a half of the scattering centers, i.e., only by the Mo d-states of the same spin. Therefore, the concentration of the Mo scattering centers is effectively lowered by half compared to the Mo doping

level. In other words, the lack of long-range magnetic order should lead to the formation of two interpenetrating networks transporting efficiently the carriers of opposite spin. Moreover, Mo population of the In(2) positions at elevated temperatures should enable the high conductivity in *both* spin channels since both the majority and minority Mo d-states are pushed away from E_F, Fig. 1(b).

Because the interstitial oxygen significantly suppresses the magnetic interactions, Table 1, the optimum transport properties can be achieved at intermediate oxygen concentration. As discussed above, the interstitial oxygen increases the relaxation time by reducing the average charge of the substitutional complexes (note the decrease of the density of states peak at E_F upon introduction of O_i which binds two electrons and forms a new band at the top of the valence band, cf., Figs. 1(a) and 1(c)). On the other hand, the magnetic exchange interactions should be strong enough to split the transition metal d-states in order to provide conductivity in one or both spin channels.

Burstein-Moss (BM) shift. To illustrate how the transition metal doping alters the electronic band structure of the host material and to compare the changes with the traditional Sn-doped case, we also calculated the band structures of pure and 6.25% Sn-doped In_2O_3. The resulting band structure plots are presented in Fig. 2. In addition, we compare the calculated fundamental band gaps $E_g(0)$, the Fermi wave vectors k_F and the plasma frequencies ω_p [21] in Table I. Most significantly, we found that the BM shift (i.e., the displacement of E_F above the conduction band minimum upon doping) is less pronounced in the IMO case – despite the fact that, at the same doping level, Mo^{6+} donates two extra carriers as compared to Sn^{4+}. This can be clearly seen from a comparison of k_F for the $Mo^{\bullet\bullet\bullet}_{In(1)}$ and $Sn^{\bullet}_{In(1)}$ structures. (Note, that unlike IMO, the doping with Sn results in k_F and ω_p to be similar to those found from the rigid-band shift in pure In_2O_3.) Such a low sensitivity to doping appears from the resonant Mo d-states located at E_F that facilitates the d-band filling and thus hinders further displacement of E_F deep into the conduction band.

Effective mass and optical properties. Smaller BM shift in IMO arising from the electron localization on the Mo d-orbitals (pinning) leads to the following advantageous features to be compared to those of ITO:

(i) Smaller increase in the effective mass is expected upon Mo doping. In addition, the Mo d-states do not hybridize with the s-states of indium which form the highly disperse conduction band. Therefore, in contrast to ITO with the strong hybridization between In and Sn s-states [14], the resonant Mo d-states at E_F do not affect the dispersion of the conduction band and hence the effective mass remains similar to the one of pure indium oxide. This is borne out in experimental observations [8] showing that the effective mass does not vary with doping (up to 12 % of Mo) and/or carrier concentration.

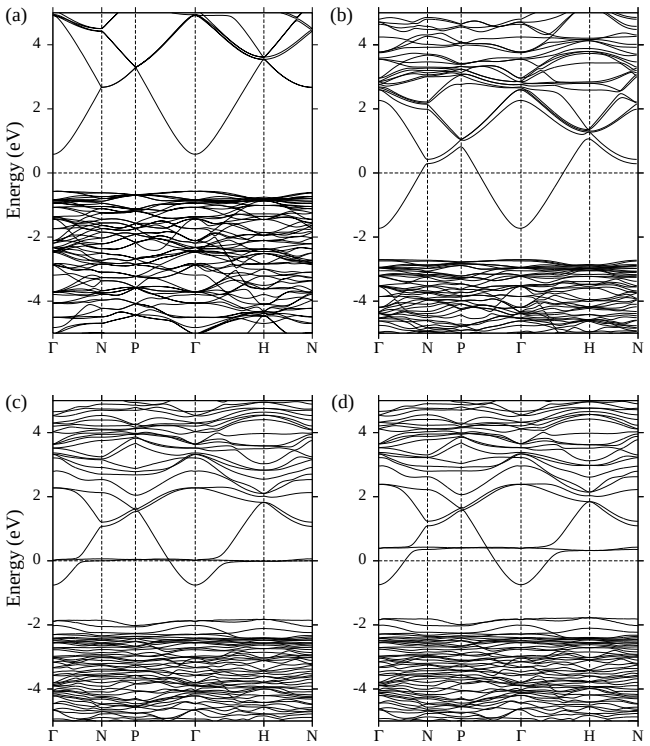

FIG. 2: Band structure for (a) pure In_2O_3, (b) $Sn^{\bullet}_{In(1)}$ structure, and (c) the majority spin and (d) the minority spin channels of $[Mo^{\bullet\bullet\bullet}_{In}O_i^{''}]^{\bullet}$ structure.

(ii) Smaller BM shift does not lead to the appearance of the intense interband transitions from the valence band in the visible range since the optical band gap in pure indium oxide is large enough, namely 3.6 eV [22]. Furthermore, in contrast to ITO where $E_g(0)$ narrowing has been demonstrated both experimentally [22] and theoretically [14], doping with Mo shows an opposite (beneficial) trend: we found that $E_g(0)$ increases upon introduction of Mo by 19 % and 9 % for $Mo^{\bullet\bullet\bullet}_{In(1)}$ and $[Mo^{\bullet\bullet\bullet}_{In}O_i^{''}]^{\bullet}$, respectively, while in the case of Sn it decreases by 16 % – as compared to pure In_2O_3 (Table I). We believe that the widening of $E_g(0)$ appears from the anisotropic d-orbitals of Mo which, in contrast to spherical s-orbitals of Sn, rotate the p-orbitals of the oxygen neighbors. As a result, the overlap of these p-orbitals with the In s-states increases, leading to the widening of $E_g(0)$.

(iii) Larger (in energy) optical transitions from the partially occupied band, i.e. from E_F, up into the conduction band (cf., Figs. 2(b) and 2(c,d)) along with the fact that transitions from d- to s-states are forbidden ensure lower short-wavelength optical absorption [23].

(iv) The calculated ω_p in IMO is below the visible range and significantly smaller than that of ITO (Table I). This finding suggests a possibility to introduce larger carrier concentrations without sacrificing the optical transmittance in the long wavelength range.

Complex	ΔE_{tot}	M	$E_g(0)$	k_F^Σ	k_F^Λ	k_F^Δ	ω_p
$Mo_{In(1)}^{\bullet\bullet\bullet}$	563	1.85	1.38	0.152	0.148	0.157	1.63
$Mo_{In(2)}^{\bullet\bullet\bullet}$	370	1.32	1.18	0.194	0.187	0.201	2.05
$[Mo_{In}^{\bullet\bullet\bullet}O_i^{''}]^{\bullet}$	32	0.50	1.26	0.125	0.123	0.132	1.27
$[Mo_{In(2)}^{\bullet\bullet\bullet}+2InO_i^{''}]^{\bullet}$	112	0.61	1.06	0.120	0.118	0.123	1.24
$Sn_{In(1)}^{\bullet}$			0.98	0.201	0.203	0.205	2.29
In_2O_3+$e^{'}$			1.16	0.206	0.204	0.213	2.38

TABLE I: The total energy differences ΔE_{tot} between nonmagnetic and ferromagnetic configuration, in meV; the magnetic moments, M, on the Mo atoms, in μ_B; the fundamental band gap values $E_g(0)$, in eV; the Fermi wave vectors k_F, in atomic units, along the [110](Σ), [111](Λ) and [010](Δ) directions; and the plasma frequency ω_p, in eV, for the different substitutional complexes with 6.25% Mo doping level. Calculated values for pure (rigid-band model) and 6.25% Sn-doped In_2O_3 are also given.

Finally, we found that the interstitial oxygen results in a decrease of both $E_g(0)$ and BM shift (Table I) – in agreement with the observed decrease of the optical band gap with ambient oxygen content [9]. Nevertheless, the optical band gap remains well above the visible range. Moreover, our calculations suggest that the overall transmittance should increase with oxygen concentration due to the increased energy of the interband transitions from E_F (smaller BM shift) and the lower plasma frequency.

In summary, using IMO as an example, we demonstrate that the transition metal dopants can be highly beneficial in providing the transport and optical properties which compete with those of commercial TCO materials. Our detailed first-principles investigations reveal the intricate role of magnetic interactions in determining both the electrical conductivity and the BM shift which in turn governs optical absorption in the visible range. Furthermore, additional calculations of In_2O_3 doped with W and 3d-elements [19] show that similar behavior can be observed in other systems leading to a family of efficient transparent conductors mediated by magnetic interactions. Recent experiments [24] support this conclusion. We expect that a variety of the appealing features in the electronic band structure arising from the electronic configuration of a proper transition metal dopant and a strong sensitivity of the d-states to the oxygen surrounding will allow control over the transport and optical properties of these advanced TCO materials.

Author acknowledges J. Tate for stimulating discussions. The work is supported by the University of Missouri Research Board.

* E-mail:juliaem@umr.edu

[1] G. Thomas, Nature, **389**, 907 (1997).

[2] D. S. Ginley and C. Bright (Eds.), Mater. Res. Bull. **25**, 15 (2000), and articles therein.

[3] S. Stoute, Mater. World, **11**, 12 (2003).

[4] T.J. Coutts, D.L. Young, and X. Li, Mater. Res. Bull. **25**, 58 (2000).

[5] J.E. Medvedeva, and A.J. Freeman, Europhys. Lett. **69**, 583 (2005).

[6] Y. Meng, X. Yang, H. Chen, J. Shen, Y. Jiang, Z. Zhang, and Z. Hua, Thin Solid Films **394**, 219 (2001); J. Vac. Sci. Technol. A **20**, 288 (2002).

[7] Y. Yoshida, T.A. Gessert, C.L. Perkins, and T.J. Coutts, J. Vac. Sci. Technol. A **21**, 1092 (2003); C. Warmsingh, *et al*, J. Appl. Phys. **95**, 3831 (2004).

[8] Y. Yoshida, D.M. Wood, T.A. Gessert, and T.J. Coutts, Appl. Phys. Lett. **84**, 2097 (2004).

[9] S. Sun, J. Huang, D. Lii, J. Vac. Sci. Technol. A **22**, 1235 (2004); J. Mater. Res., **20**, 247 (2005).

[10] Y. Yang, *et al*, J. Amer. Chem. Society **127**, 8796 (2005).

[11] E. Wimmer, H. Krakauer, M. Weinert, and A.J. Freeman, Phys. Rev. B **24**, 864 (1981).

[12] Cut-offs of the plane-wave basis (16.0 Ry) and potential representation (81.0 Ry), and expansion in terms of spherical harmonics with $\ell \leq 8$ inside the muffin-tin spheres were used. Summations over the Brillouin zone were carried out using 24 special **k** points in the irreducible wedge.

[13] M. Marezio, Acta Cryst. **20**, 723 (1966).

[14] O.N. Mryasov and A.J. Freeman, Phys. Rev. B **64**, 233111 (2001).

[15] N. Nadaud, N. Lequeux N, M. Nanot, J. Love, and T. Roisnel, J. Solid State Chem. **135**, 140 (1998).

[16] The formation energy is calculated as $E_f = E_{In_2O_3:Mo} - E_{In_2O_3} - E_{In} + E_{Mo}$, where $E_{In_2O_3:Mo}$, $E_{In_2O_3}$, E_{In}, and E_{Mo} are the total energy of the Mo-doped and the corresponding undoped indium oxide, and bulk bct In and bcc Mo, respectively. For the structures with interstitial oxygen, the E_f was calculated in two ways: via the total energy of indium oxide with an additional oxygen, i.e., $E_f = E_{In_2O_3:MoO_i} - E_{In_2O_3:O_i} - E_{In} + E_{Mo}$ and the total energy of the oxygen molecule O_2, i.e., $E_f = E_{In_2O_3:MoO_i} - E_{In_2O_3} - E_{In} + E_{Mo} + E_{O_2}/2$.

[17] This is in contrast to ITO, where interstitial oxygen observed experimentally [18] results in the formation of neutral defect complexes, $[2Sn_{In}^{\bullet}O_i^{''}]^x$. In IMO, neutral complexes may arise from $[2Mo_{In}^{\bullet\bullet\bullet}3O_i^{''}]^x$. Another possibility is that Mo may also exist in the valence state of 4+ which may lead to the formation of $[2Mo_{In}^{\bullet}O_i^{''}]^x$ complexes. Studies of the neutral complexes are beyond the scope of this work.

[18] A.J. Freeman, K.R. Poeppelmeier, T.O. Mason, R.P.H. Chang, and T.J. Marks, Mater. Res. Bull. **25**, 45 (2000); G.B. González, *et al*, J. Appl. Phys. **89**, 2550 (2001).

[19] J.E. Medvedeva, unpublished.

[20] Weak coupling between the dopants makes it hard to detect the magnetic properties experimentally.

[21] The plasma frequency was estimated using the Eq. (1) in Ref. [14] via the calculated Fermi wave vectors and Fermi group velocities.

[22] I. Hamberg, *et al*, Phys. Rev. B **30**, 3240 (1984).

[23] Our results show that the second (hybridization) gap which was argued to be one of the reasons of low optical absorption in ITO [14] closes upon structural relaxation.

[24] P.F. Newhouse, C.-H. Park, D.A. Keszler, J. Tate, and P.S. Nyholm, Appl. Phys. Lett. **87**, 112108 (2005).